A Study of Optimized-LQR Control for Rotary Inverted Pendulum by Particle Swarm Optimization

Thanh-Tri-Dai Le [1], Thanh-Cong Pham [2,*], Duc-Thanh-Long Bui [3], Quang-Truong Nguyen [4], Van-Nhat-Truong Vo [5], Quoc-Lap Dinh [6], Le-Hieu Tran [7], Thien-Bao Truong [8], Tan-Loc Nguyen [9], Duy-Tan Nguyen [10], Tuan-Anh Nguyen [11], Viet-Anh Nguyen [12], Thi-Thanh-Hoang Le [13]

[1] Faculty of International Training, Ho Chi Minh City University of Technology and Education (HCMUTE), Ho Chi Minh City (HCMC), Vietnam

[2, 3, 4, 5, 6, 7, 10, 11, 12, 13] Faculty of Electrical and Electronics Engineering (FEEE), Ho Chi Minh City University of Technology and Education (HCMUTE), Ho Chi Minh City (HCMC), Vietnam

[8, 9] Faculty of Mechanical Engineering, Ho Chi Minh City University of Technology and Education (HCMUTE), Ho Chi Minh City (HCMC), Vietnam

Email: [1] 19151051@student.hcmute.edu.vn, [2] 17151175@student.hcmute.edu.vn, [3] 20161222@student.hcmute.edu.vn, [4] 20161286@student.hcmute.edu.vn, [5] 20161029@student.hcmute.edu.vn, [6] 20161025@stuednt.hcmute.edu.vn, [7] 20161193@student.hcmute.edu.vn, [8] 21146428@student.hcmute.edu.vn, [9] 21146125@student.hcmute.edu.vn, [10] 20161257@student.hcmute.edu.vn, [11] 21143326@student.hcmute.edu.vn, [12] 20161156@student.hcmute.edu.vn, [13] hoangltt@hcmute.edu.vn

*Corresponding Author

***Abstract*—Rotary Inverted Pendulum (RIP) is a classical but effective model in testing control algorithms. Besides designing controllers, it can also be a model for testing the evolution algorithms (EAs) in optimizing control parameters. In this paper, we apply particle swarm optimization (PSO), which is an EA, to optimize the parameters of the LQR controller for this model. In the study, an experimental model in which system parameters are already measured and identified in former studies is used. The LQR control method is inherited from former results, and the weighing matrices (Q and R) are optimized by the PSO method. In each case, the control matrix K is obtained from Q and R to apply for RIP. Through both simulation and experiment, LQR control parameters are found better through generations by using PSO. The responses of RIP, in which controllers are designed under optimized Q and R in later generations, are better in quality, and values of the fitness function also supports that opinion. Thence, through this study, beside genetic algorithm (GA), this study proves that PSO is a suitable searching algorithm that can be applied for balancing this single input- multi output (SIMO) system. Also, the experimental platform of RIP in this research confirms its ability to control tests.**

***Keywords*—PSO; Genetic Algorithm; Rotary Inverted Pendulum; SIMO System**

I. INTRODUCTION

SIMO system [1] is a class of systems controlled by one control signal when controlling more than one variable. Those models are usually balanced robots. Among them, RIP [2] is a popular SIMO model in control engineering. It has a simple structure but a highly nonlinear feature. Thence, it becomes a classical model in training and research activities in a control laboratory. Due to its popularity, it has become a standard model that is industrially produced by Quanser for laboratories [3]. Some other similar kinds of inverted pendulum (IP) developed from RIP are: cart and pole [4], double-linked RIP, which is created by adding one more parallel link [5] or serial link [6]. Thence, any study from standard RIP can be developed for those similar models.

Based on this model, PID [7], pole-placement [8], sliding control [9] methods are tested well. The control methods are examined in many papers, with control parameters chosen through trial-and-error. To automatically search these parameters, evolution algorithms (EAs) are developed [10]. GA is the most popular algorithm in EAs. It was proved to optimize well controllers for the heating oven [11], DC motor [12]. In [13], GA is proved to be effective for finding PID control parameters for an antenna system. It is also applied well in parameter searching for nonlinear algorithms, such as back-stepping [14]. However, proving the ability to optimize control parameters for a linear controller is still necessary. In [15], PSO is also regarded to be more effective than GA in theory. However, Experimental results are still necessary.

In [14], we created an experimental RIP in which back-stepping control is tested well in both simulation and experiment. Thence, it becomes our main model for researching. In this paper, we apply LQR control again for this model and use PSO to examine the effectiveness of PSO on optimizing LQR control.

II. MATHEMATICAL MODEL

From [14], mathematical model of RIP is described in Fig. 1. Also, the features of the experimental model are shown in Table 1, (1), (2).

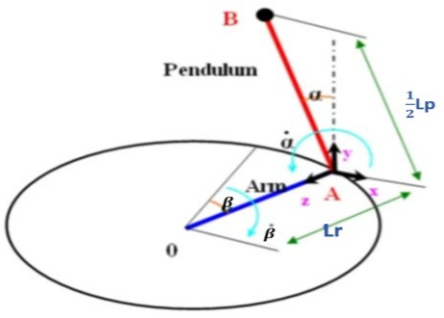

Fig. 1. Mathematical model of RIP

Table 1. System parameters

Symbols	Description
α	Angle of pendulum(rad)
β	Angle of arm (rad)
m_p	Mass of pendulum (kg)
L_p	Length of pendulum (m)
J_p	Inertia moment of pendulum (kgm^2)
m_r	Mass of arm (kg)
L_r	Length of arm (m)
J_r	Inertia moment of arm (kgm^2)
g	Gravitational acceleration (m/sec^2)
M_{en}	Mass of encoder measuring α (kg)
e	Voltage on DC motor (V)
R_m	Resistor of motor (Ω)
L_m	Inductance of motor (H)
K_b	Counter electromotive constant (V/rad/sec)
K_t	Moment constant (Nm/A)
J_m	Moment of inertia of DC motor rotor (kgm^2)
C_m	Viscous coefficient of friction (Nm/rad/sec)
T_f	Frictional torque (Nm)

The values of system parameters are

$$L_r = 0.2;\ M_{en} = 0.2;\ M_p = 0.09;\ M_r = 0.04872;\\ L_p = 0.25;\ K_t = 0.0861;\\ C_m = 0;\%6.74 * (10^{-5});\ K_b = 0.0861;\\ R_m = 11.9444;\ J_m = 5.98 * (10^{-5});\ g = 9.81 \quad (1)$$

The dynamic equations of RIP are:

$$\dot{x} = f(x, e) \quad (2)$$

where

$$f(x,e) = f = [f_1 \quad f_2 \quad f_3 \quad f_4]^T;$$
$$x = [x_1 \quad x_2 \quad x_3 \quad x_4]^T$$
$$f_1 = x_2;\ f_3 = x_4;\ K_1 = \frac{K_t}{R_m};\ K_2 = C_m + \frac{K_t}{R_m}K_b;\ K_3 = J_m$$
$$f_2 = \frac{3\begin{pmatrix}6\,K_3 g\sin x_1 - 6K_2 L_r \dot{\beta}\cos x_1 + 6K_1 L_r e\cos x_1 + \\ +6L_r^2 M_{en} g\sin x_1 + 6L_r^2 M_p g\sin x_1 + 2L_r M_r g\sin x_1 + \\ -3L_p L_r^2 M_p x_2^2 \cos x_1 \sin x_1\end{pmatrix}}{L_p\begin{pmatrix}12K_3 + 12L_r^2 M_{en} + 12L_r^2 M_p + \\ +4L_r^2 M_r - 9L_r^2 M_p \cos^2 x_1\end{pmatrix}};$$
$$f_4 = \frac{3\begin{pmatrix}4L_p L_r M_p \sin x_1 x_2^2 + 4K_2\dot{\beta} + \\ -4K_1 e - 3L_r M_p g\cos x_1 \sin x_1\end{pmatrix}}{\begin{pmatrix}12K_3 + 12L_r^2 M_{en} + 12L_r^2 M_p + \\ +4L_r^2 M_r - 9L_r^2 M_p \cos^2 x_1\end{pmatrix}}$$

III. ALGORITHM

A. LQR control

Voltage on DC motor – control signal- under the LQR method is calculated as

$$e = u = -Kx \quad (3)$$

where K is the control matrix. The structure of control is shown in Fig. 2.

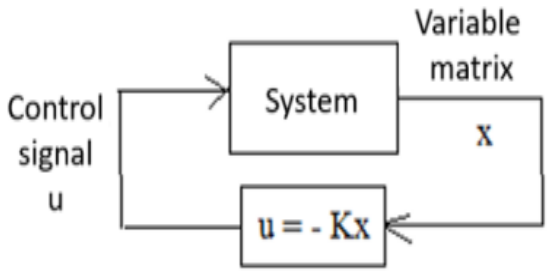

Fig. 2. Structure of LQR for RIP

Linear model of (2) at the equilibrium point is

$$\dot{x} = Ax + Bu \quad (4)$$

where $A = \left[\begin{matrix}\frac{\partial f_1}{\partial x_1} & \frac{\partial f_1}{\partial x_2} & \frac{\partial f_1}{\partial x_3} & \frac{\partial f_1}{\partial x_4}\\ \frac{\partial f_2}{\partial x_1} & \frac{\partial f_2}{\partial x_2} & \frac{\partial f_2}{\partial x_3} & \frac{\partial f_2}{\partial x_4}\\ \frac{\partial f_3}{\partial x_1} & \frac{\partial f_3}{\partial x_2} & \frac{\partial f_3}{\partial x_3} & \frac{\partial f_3}{\partial x_4}\\ \frac{\partial f_4}{\partial x_1} & \frac{\partial f_4}{\partial x_2} & \frac{\partial f_4}{\partial x_3} & \frac{\partial f_4}{\partial x_4}\end{matrix}\right]_{\substack{x=0\\u=0}}$; $B = \left[\begin{matrix}\frac{\partial f_1}{\partial u}\\ \frac{\partial f_2}{\partial u}\\ \frac{\partial f_3}{\partial u}\\ \frac{\partial f_4}{\partial u}\end{matrix}\right]_{\substack{x=0\\u=0}}$

With system parameters in (1), matrices A, B are

$$A = \begin{bmatrix}0 & 1 & 0 & 0\\ 75.3981 & 0 & 0 & -0.0860\\ 0 & 0 & 0 & 1\\ 13.7818 & 0 & 0 & -0.0717\end{bmatrix};\ B = \begin{bmatrix}0\\ 0.9008\\ 0\\ 0.7507\end{bmatrix} \quad (5)$$

Thence, matrix K in (3) is calculated by solving the Riccati equation. However, we can use the command $lqr()$ in MATLAB to easily obtain this matrix as

$$K = lqr(A, B, Q, R) \quad (6)$$

Q and R are weighing matrices that should be chosen.

B. PSO

Position change model of the PSO algorithm in space is shown in Fig. 3.

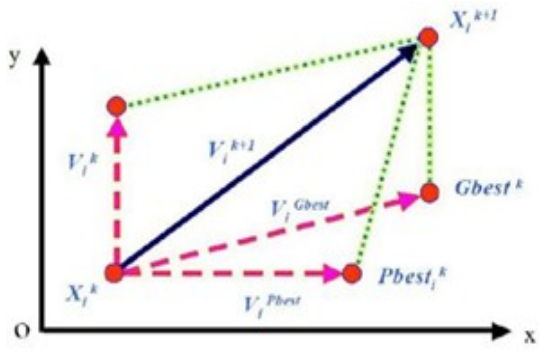

Fig. 3. The principle of changing the position of an individual in a 2-dimensional space

Fundamentals of PSO technique are stated and defined as follows:

Individual $X(i)$: Is a candidate solution represented by a k-dimensional real-valued vector, where k is the number of

optimized parameters. At iteration i, the position of the jth individual $X(i,j)$ can be described as follows:

$$X_j(i) = [x_{j,1}(i); x_{j,2}(i); \ldots; x_{j,k}(i); \ldots; x_{j,d}(i)] \quad (7)$$

where $xk(i,j)$ is k[th] optimal parameter in j[th] candidate solution; d represents the control variables.
Population: is set of n individuals at i[th] iteration

$$pop(i) = [X_i(i), X_2(i), \ldots, X_n(i)]^T \quad (8)$$

where n stands for the number of candidate solutions.
A swarm is an unorganized population of mobile individuals that tend to gather together while each individual tends to move in a random direction.

Individual velocity $V(i)$: is the velocity of the moving individual, represented by a d-dimensional real-valued vector. At iteration i[th], the velocity of the j[th] individual is $Vj(i)$, which can be described as follows:

$$V_j(i) = [v_{j,1}(i); v_{j,2}(i); \ldots; v_{j,k}(i); \ldots v_{j,d}(i)] \quad (9)$$

With $vj,(i)$ being the velocity component of the j[th] individual in the k[th] dimensional space.

Best Individual $X*(i)$: During the movement of an individual through the search space, it compares the fitness values at its current position with the fitness values it has achieved previously at any iteration up to the current iteration. The best position that is associated with the best fitness value achieved is called the best individual $X*(i)$. For each individual in the swarm, $X*(i)$ can be determined and updated during the search. The j[th] individual, the best individual, can be expressed as follows:

$$X_{j*}(i) = [x_{j,1*}(i), x_{j,2*}(i), \ldots x_{j,d*}(i)]^T \quad (10)$$

In a minimization problem with a single objective function f, the jth best individual $Xj*(i)$ is updated whenever $(Xj*(i)) < (Xj*(i-1))$

Iteration Stopping Criteria: The search process will terminate when one of the following criteria is satisfied:

- The number of iterations since the last change of the best solution is greater than a previously specified number.
- The number of iterations reaches the maximum allowed number.

The velocity of the individual in the k[th] dimension is limited by some maximum value vk_{max}. This limit extends the local exploration of the problem space, and it effectively simulates the larger variation of human learning. The maximum velocity in the k[th] dimension is described by a sequence of k[th] optimal parameters and is given by:

$$v_k^{max_k^{min}} \quad (11)$$

The diagram of applying PSO in optimizing the controller is shown in Fig. 4.

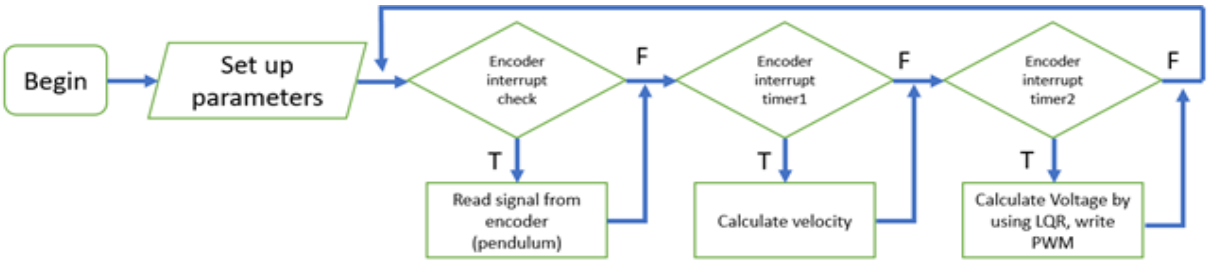

Fig. 4. PSO optimizing diagram

IV. Results and Discussion

A. Real Model

The real model is shown in Fig. 5. It is re-utilized, and the system parameters are maintained as in [14]. The description of components in Fig. 5 is:

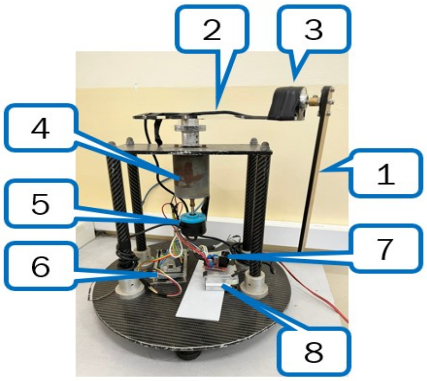

Fig. 5. Real model [14]

Information of Fig. 5 is: 1-pendulum, 2-arm, 3-encoder that measures the angle of the pendulum (α), 4-DC motor, 5-encoder that measures the angle of the arm (β), 6-STM32 control chip, 7-L298 H-bridge board, 8-DC source.

B. Simulation and Experiment Program

The simulation program is described in Fig. 6 and Fig. 7. Description of blocks in Fig. 6 is: 1-Block calculating control signal (in (3)), 2-Block imitating RIP. This block is explained in detail in Fig. 7, 3-State of variables, 4-Parts that calculate the mean square of errors. Description of blocks in Fig. 7 is: 1-Control signal of RIP (voltage on DC motor), 2-Blocks that describe the dynamic equations of RIP in (2), 3-Systems variables

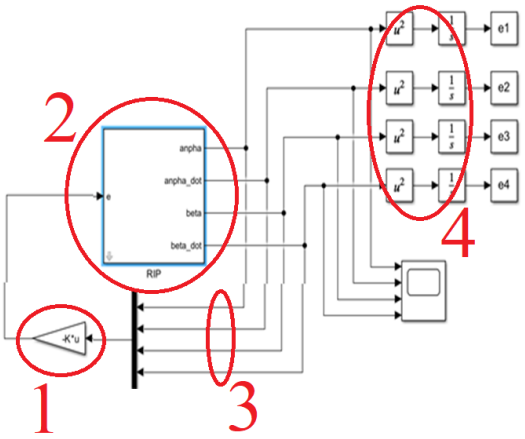

Fig. 6. Simulation program of LQR control for RIP

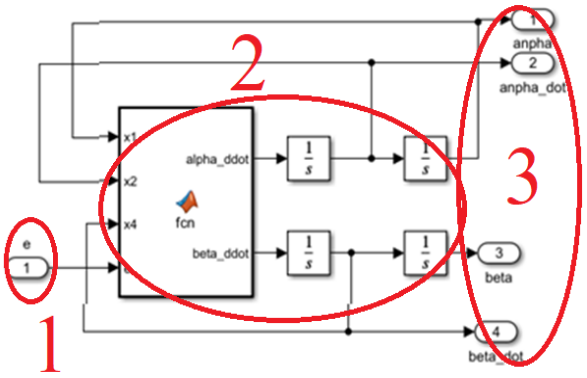

Fig. 7. Blocks describing the RIP model

The embedded program for the experimental model is described in Fig. 8 and Fig. 9. Description of blocks in Fig. 8 is: 1-Block calculating the pulse from the encoder of the arm, 2-Block calculating pulse from encoder of pendulum, 3-Value of the angle of the arm, 4-Value of the angle of the pendulum. Description of blocks in Fig. 9 is:1-Value of the angle of the arm, 2-Value of the angle of the pendulum, 3-Block that calculates the control signal through the LQR method, 4-Signal that controls the direction of the motor, 5-Signal that controls the velocity of the motor.

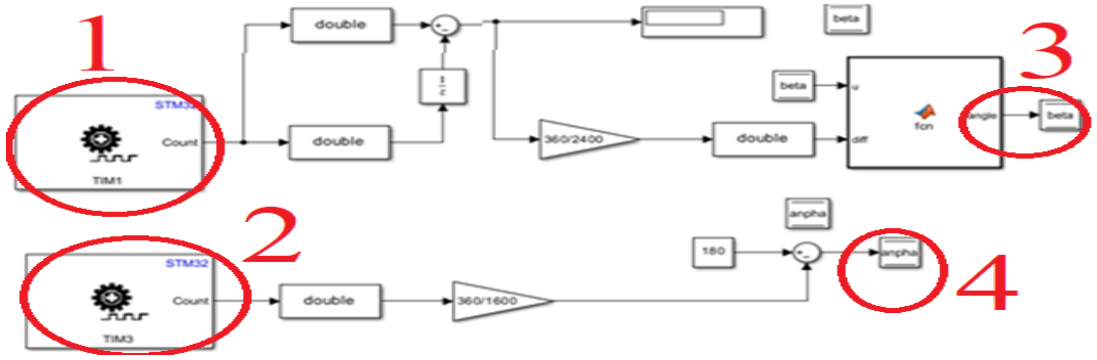

Fig. 8. Blocks describing input signals from sensors

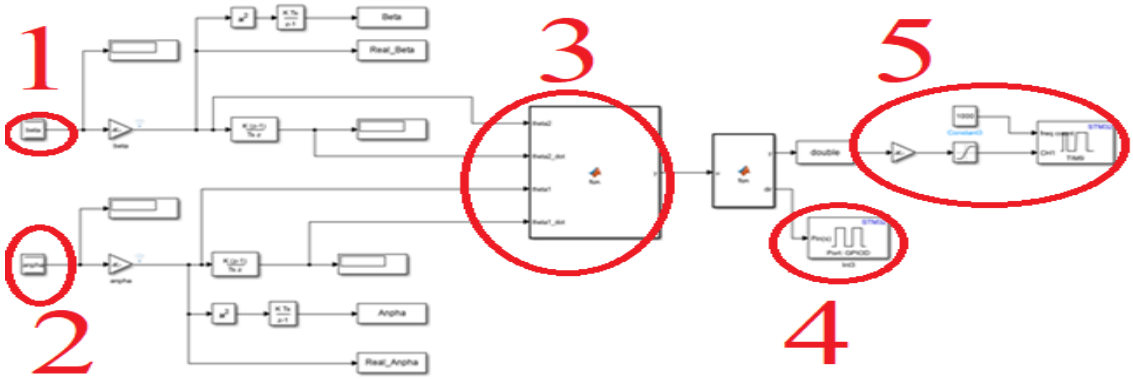

Fig. 9. Blocks describing the controller and the control signal

5.1. Standard LQR algorithm

In the simulation, the initial values of RIP are chosen as

$$\alpha = \frac{\pi}{18}(rad); \dot{\alpha} = 0.005(rad); \\ \beta = 0.1(rad); \dot{\beta} = 0; \tag{12}$$

A trial-and-error test is used to choose matrices Q and R as

$$Q = \begin{bmatrix} 600 & 0 & 0 & 0 \\ 0 & 600 & 0 & 0 \\ 0 & 0 & 800 & 0 \\ 0 & 0 & 0 & 200 \end{bmatrix}; R = 1 \tag{13}$$

Thence, from (5), (6), (13), we obtain K to get the simulation result in Fig. 10.

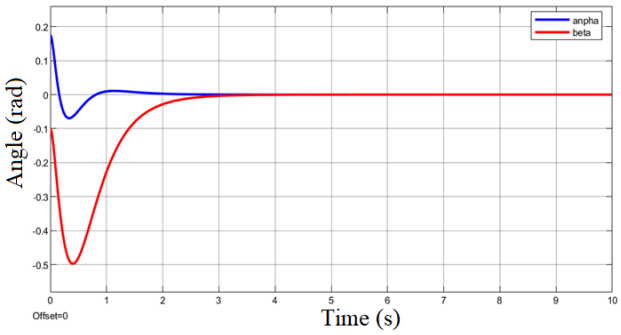

Fig. 10. Response (rad) of RIP under standard LQR control

In Fig. 10, pendulum moves from the initial position (0.2 rad) to the equilibrium point after 4sec. Then, it is balanced. Also, the arm moves from the initial value (-0.1 rad) to position (-0.5 rad) and it is stabilized at 0 position after 6 sec. Using the ISE method to evaluate the fitness of the system, considering e_1 as the error of α and e_3 as the error of β, we obtain.

$$ISE = \int ({e_1}^2 + {e_3}^2) = 445.9587 \quad (14)$$

The experimental result is shown in Fig. 11 and Fig. 12. In Fig. 11, the angle of the pendulum is stable. However, the vibration is 0.04 rad around the equilibrium point. In Fig. 12, the arm vibrates from 0.15 rad to 0.42 rad from the zero position.

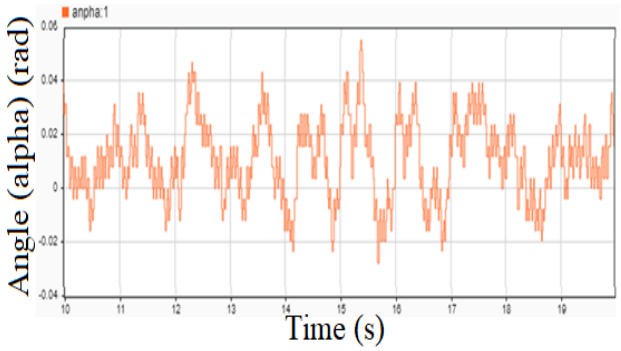

Fig. 11. Experimental angle pendulum

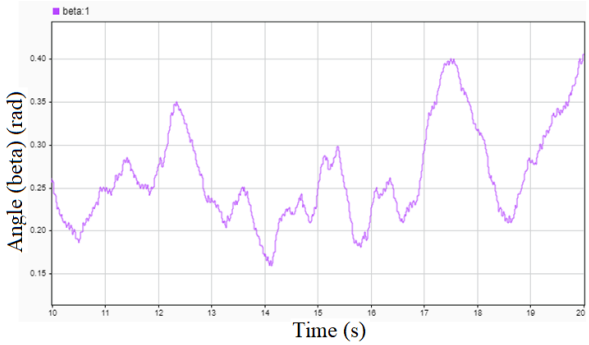

Fig. 12. Experimental angle of arm

From Fig. 11 and Fig. 12, using the ISE method to evaluate the fitness of the system, we obtain.

$$ISE = \int ({e_1}^2 + {e_3}^2) = 32663.406181 \quad (15)$$

C. *Optimized-LQR algorithm with no weighting constant*

The cost function is chosen as

$$ISE = \int ({e_1}^2 + {e_3}^2) \quad (16)$$

Limitation of components in matrices Q and R as

$$Q = [0, 5000];\ R = [1, 5] \quad (17)$$

By PSO, we obtain matrices Q and R as

$$Q = \begin{bmatrix} 5000 & 0 & 0 & 0 \\ 0 & 5000 & 0 & 0 \\ 0 & 0 & 3494.31 & 0 \\ 0 & 0 & 0 & 5000 \end{bmatrix};\ R = 1 \quad (18)$$

From (5), (6), (18), we obtain the LQR controller, and the simulation and experiment are shown in Fig. 13 to Fig. 15.

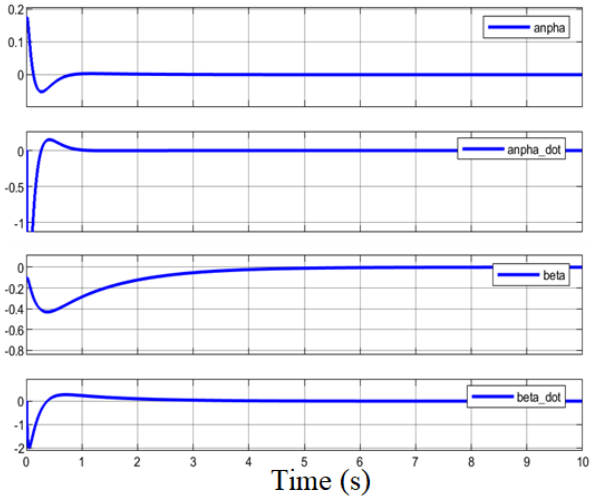

Fig. 13. Simulation results (rad and rad/s)

In Fig. 13, the settling time of angle α is about 0.8 sec, and that of angle β is about 4 sec. The cost function of the simulation results is

$$ISE = \int {e_1}^2 + {e_3}^2 = 54.2752 \quad (19)$$

In Fig. 14, the pendulum oscillates around the equilibrium position. Pendulum oscillates around 0.05 (rad) to -0.03 (rad). The settling value is around 0.01 (rad). In Fig. 15, arm oscillates from 0.2 (rad) to 0.55 (rad). The cost function in the experiment is

$$ISE = \int {e_1}^2 + {e_3}^2 = 18301 \quad (20)$$

From (14) and (17) (ISE of simulation), from (15) and (20), the cost function in the case using PSO is smaller than

the non-PSO results. Thence, PSO successfully optimizes LQR control in simulation and experiment

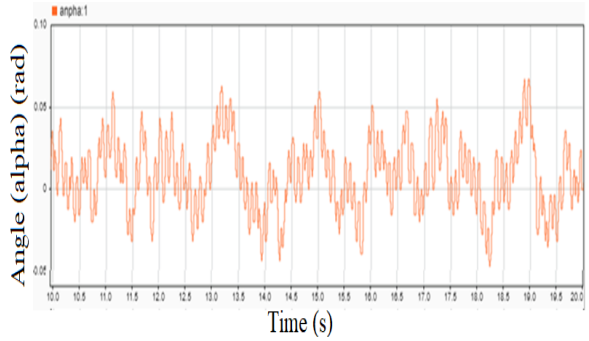

Fig. 14. Angle of pendulum

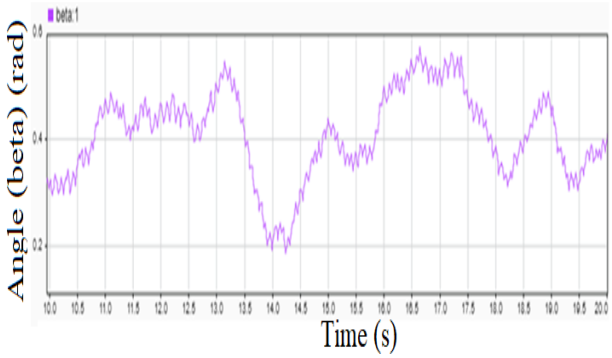

Fig. 15. Angle of arm

D. Optimized-LQR algorithm with weighting constant

1) The Cost function is chosen as

$$ISE = \int (x{e_1}^2 + {e_3}^2) \quad (21)$$

where x is a weighing constant

Limitation of components in Q and R, the value of x is chosen as

$$Q = [0, 5000];\ R = [1, 5]\ and\ x = 640 \quad (22)$$

Thence, PSO give us the values of Q and R as

$$Q = \begin{bmatrix} 5000 & 0 & 0 & 0 \\ 0 & 580.98213 & 0 & 0 \\ 0 & 0 & 1062.329 & 0 \\ 0 & 0 & 0 & 5000 \end{bmatrix};\ R = 1 \quad (23)$$

Thence, the control results are shown in Fig 16 to Fig. 18. In Fig. 17, pendulum oscillates around the equilibrium position. The pendulum oscillates around 0.06 (rad) to -0.04 (rad), and the average value is around 0.01 (rad). When adding a weighing constant x to e_1 in the cost function, the vibration of the pendulum is smaller (in Fig. 14 and Fig. 17). And, the quality control of the arm is not considered (in Fig. 15 and Fig. 18).

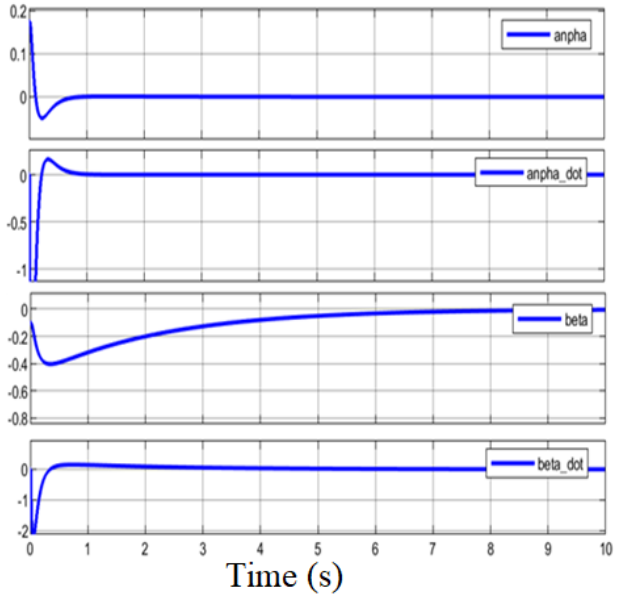

Fig. 16. Simulation response (rad and rad/s)

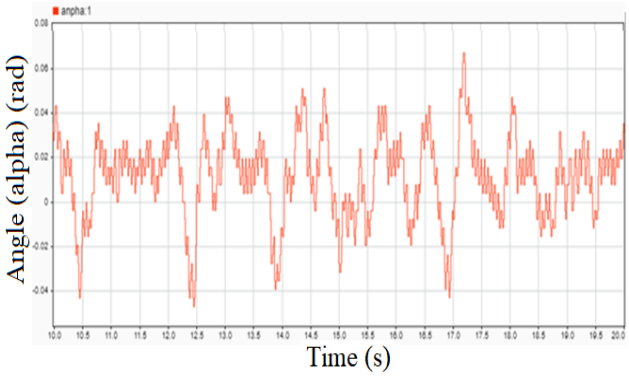

Fig. 17. Angle of pendulum

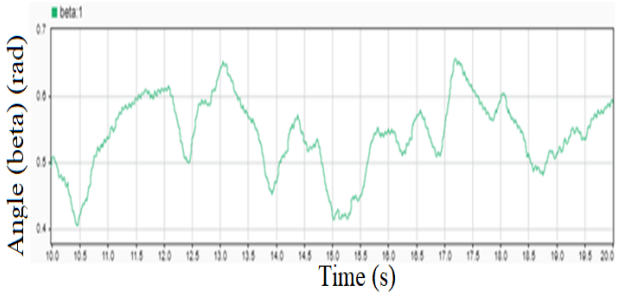

Fig. 18. Angle of arm

2) The cost function is chosen as

$$ISE = \int ({e_1}^2 + x{e_3}^2) \quad (24)$$

Limitation of components in Q and R, the value of x is chosen as

$$Q = [0, 5000];\ R = [1, 5]\ and\ x = 640 \quad (25)$$

Thence, PSO gives us the values of Q and R as

$$Q = \begin{bmatrix} 5000 & 0 & 0 & 0 \\ 0 & 1 & 0 & 0 \\ 0 & 0 & 5000 & 0 \\ 0 & 0 & 0 & 19.4276 \end{bmatrix}; \; R = 1 \qquad (26)$$

Thence, the control results are shown in Fig. 19. In Fig. 20, the pendulum oscillates around the equilibrium position. The pendulum oscillates around 0.05 (rad) to -0.04 (rad), and the average value of the oscillation is around 0.01 (rad). In Fig. 21, the arm ranges from 0.03 (rad) to 0.18 (rad). In Fig. 15 and Fig. 21, when adding the weighing constant x in (25), quality control of the arm is smaller (less vibration). Thence, weighing constant helps to optimize the main component that we care about (in this case, it is β).

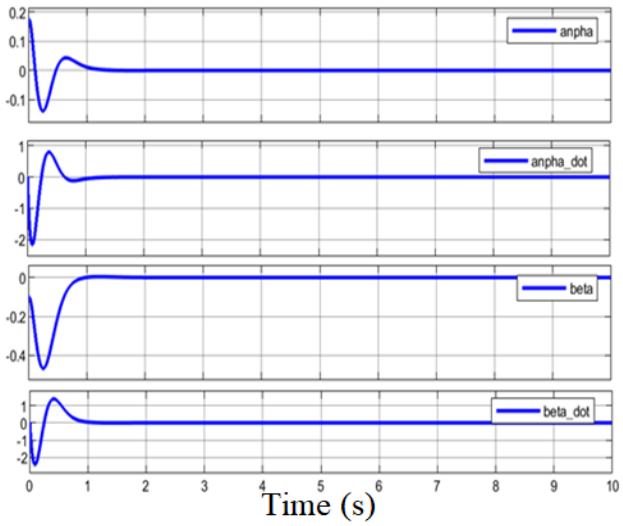

Fig. 19. Simulation response (rad and rad/s)

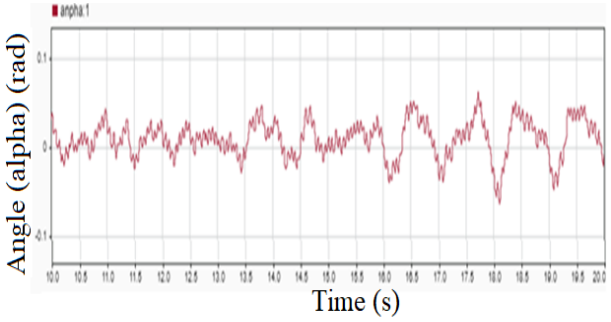

Fig. 20. Angle of pendulum

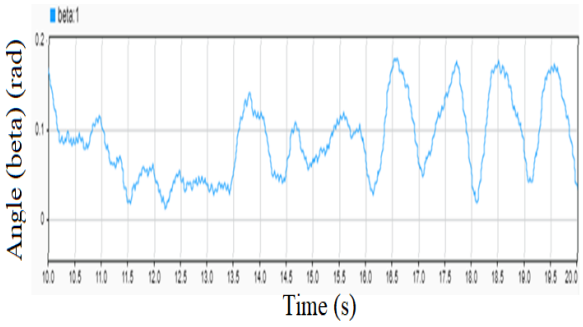

Fig. 21. Angle of arm

V. Conclusion

Through the paper, optimized-LQR controllers based on PSO make the response of a RIP better than a normal LQR controller: shorter settling time, smaller oscillation in simulation and experiment. These criteria can be described more easily by the smaller fitness function. Also, the later generations of the finding matrices Q and R give smaller fitness functions. Thence, PSO is proved to be a successful method in optimizing control parameters. In this case, they are matrices Q and R. The results are described randomly due to the uncertainty of the searching methods. PSO is proven to successfully optimize the control parameters and give better quality control (through values of cost function comparison). Thence, a constant x is added to adjust the optimization to a variable that we care. And, the study shows the method to calibrate this constant to obtain a better quality for the expected variable.

Acknowledgment

This paper belongs to a project of students of HCMUTE in 2025. It is funded by HCMUTE. We want to give thanks for this support. We also want to give thanks to PhD. Van-Dong-Hai Nguyen (FEEE-HCMUTE) for supervision of this contribution.

References

[1] S. Gezici and Z. Sahinoglu, "Ranging in a Single-Input Multiple-Output (SIMO) System," in *IEEE Communications Letters*, vol. 12, no. 3, pp. 197-199, 2008, https://doi.org/10.1109/LCOMM.2008.071691.

[2] S. Jadlovská and J. Sarnovský, "A complex overview of the rotary single inverted pendulum system," *2012 ELEKTRO*. 305-310, 2012, https://doi.org/10.1109/ELEKTRO.2012.6225609.

[3] M. Roman, E. Bobasu and D. Sendrescu, "Modelling of the rotary inverted pendulum system," *2008 IEEE International Conference on Automation, Quality and Testing, Robotics*, pp. 141-146, 2008, https://doi.org/10.1109/AQTR.2008.4588810.

[4] T.-B. Dang *et al.*, "PID Control for Cart and Pole system: Simulation and Experiment," *JFSC*, vol. 2, no. 1, pp. 29–35, 2024, https://doi.org/10.59247/jfsc.v2i1.165.

[5] C.-H. Nguyen *et al.*, "ANFIS-based LQR Control for Rotary Double Parallel Inverted Pendulum", *JFSC*, vol. 2, no. 2, pp. 109–116, 2024, https://doi.org/10.59247/jfsc.v2i2.214.

[6] N.-C. Tran *et al.*, "LQR Control for Experimental Double Rotary Inverted Pendulum", *JFSC*, vol. 2, no. 2, pp. 104–108, 2024. https://doi.org/10.59247/jfsc.v2i2.212.

[7] A. L. M, A. Kunjumuhammed, J. Tomy, U. G, M. Sivadas and A. Mohan, "Stabilization of Rotary Inverted Pendulum using PID Controller," *2021 8th International Conference on Smart Computing and Communications (ICSCC)*, pp. 376-380, 2021, https://doi.org/10.1109/ICSCC51209.2021.9528290.

[8] Fahmizal, Geonoky, and H. Maghfiroh, "Rotary Inverted Pendulum Control with Pole Placement", *JFSC*, vol. 1, no. 3, pp. 90–96, 2023, https://doi.org/10.59247/jfsc.v1i3.152.

[9] Mojtaba Ahmadieh Khanesar, Mohammad Teshnehlab and Mahdi Aliyari Shoorehdeli, "Sliding mode control of Rotary Inverted Pendulm," *2007 Mediterranean Conference on Control & Automation*, pp. 1-6, 2007, https://doi.org/10.1109/MED.2007.4433653.

[10] P. A. Vikhar, "Evolutionary algorithms: A critical review and its future prospects," *2016 International Conference on Global Trends in Signal Processing, Information Computing and Communication (ICGTSPICC)*, pp. 261-265, 2016, https://doi.org/10.1109/ICGTSPICC.2016.7955308.

[11] B. Yang *et al.*, "Optimizing PID Controller Based on Genetic Algorithm for Industrial Microwave Heating Device", *International Journal of Digital Content Technology and its Applications*, vol. 6, no. 23, pp. 475-483, 2012, https://doi.org/10.4156/jdcta.vol6.issue23.54.

[12] S. Tiwari *et al.*, "Control of DC Motor Using Genetic Algorithm Based PID Controller," *2018 International Conference and Utility Exhibition on Green Energy for Sustainable Development (ICUE)*, pp. 1-6, 2018, https://doi.org/10.23919/ICUE-GESD.2018.8635662.

[13] B.-H. Nguyen *et al*., "Application of Genetic Algorithm for Optimizing Continuous and Discrete PID to Control Antenna Azimuth Position", *JFSC*, vol. 2, no. 1, pp. 1–5, 2024, https://doi.org/10.59247/jfsc.v2i1.154.

[14] H.-G.-B. Pham *et al*, "Trajectories Tracking Control for Rotary Inverted Pendulum using Back-stepping Method", *JFSC*, vol. 3, no. 1, pp. 57–63, 2025, https://doi.org/10.59247/jfsc.v3i1.276.

[15] T. M. Shami *et al.*, "Particle Swarm Optimization: A Comprehensive Survey," in *IEEE Access*, vol. 10, pp. 10031-10061, 2022, https://doi.org/10.1109/ACCESS.2022.3142859.